HAL
open science

Numerical experiments using mesonh/forefire coupled Atmospheric-fire model

Jean Baptiste Filippi, Frédéric Bosseur, Céline Mari, Susanna Strada

To cite this version:

Jean Baptiste Filippi, Frédéric Bosseur, Céline Mari, Susanna Strada. Numerical experiments using mesonh/forefire coupled Atmospheric-fire model. Eighth Symposium on Fire and Forest Meteorology, Oct 2009, Kalispell, United States. pp.9. hal-00593597

HAL Id: hal-00593597

https://hal.science/hal-00593597v1

Submitted on 16 May 2011

HAL is a multi-disciplinary open access archive for the deposit and dissemination of scientific research documents, whether they are published or not. The documents may come from teaching and research institutions in France or abroad, or from public or private research centers.

L'archive ouverte pluridisciplinaire **HAL**, est destinée au dépôt et à la diffusion de documents scientifiques de niveau recherche, publiés ou non, émanant des établissements d'enseignement et de recherche français ou étrangers, des laboratoires publics ou privés.

7.3

NUMERICAL EXPERIMENTS USING MESONH/FOREFIRE COUPLED ATMOSPHERIC-FIRE MODEL

Jean Baptiste Filippi [1], Frédéric Bosseur [1], Céline Mari [2], Suzanna Stradda [2]
[1] SPE - CNRS UMR 6134, Campus Grossetti, BP52, 20250 Corte
[2] LA - CNRS UMR 5560, OMP, 14 Avenue Edouard Belin, 31400 Toulouse

In this study we attempt to couple the MesoNH atmospheric model in its large eddy simulation configuration with a fire contour model, ForeFire. Coupling is performed at each atmospheric time step, with the fire propagation model inputting the wind fields and outputting heat and vapour fluxes to the atmospheric model.
ForeFire model is a Lagrangian front tracking model that runs at a typical front resolution of 1 meter. If the approach is similar to other successful attempts of fire-atmosphere coupled models, the use of MesoNH and ForeFire implied the development of an original coupling method. Fluxes outputted to the atmospheric models are integrated using polygon clipping method between the fire front position and the atmospheric mesh. Another originality of the approach is the fire rate of spread model that integrates wind effect by calculating the flame tilt. This reduced physical model is based on the radiating panel hypothesis. A set of idealized simulation are presented to illustrate the coupled effects between fire and the atmosphere. Preliminary results show that the coupled model is able to reproduce results that are comparable to other existing numerical experiments with a relatively small computational cost (one hour for a typical idealized case on a 200 GFlops capable computer). MesoNH serves as a research model for the meteorological systems in France and Europe, and is well integrated within the operational tool chain. Future validation scenarios will be performed on nested simulations of real large wildfires.

Keywords:
Fire spread, wildland, fire, coupled atmosphere-fire numerical model.

1. Introduction

Fire behaviour is dependent of many physical processes; modelling interaction between all these processes would require a highly detailed and computationally intensive model. Moreover, it is rarely possible to gather sufficient data to initiate a simulation at the level of detail required for such simulations. Nevertheless, fire area simulator, such as FARSITE, are of a prime interest to the people who fight wildfires, and taking into account more of these coupled physical effects may permit to enhance the performance of such models. The proposed approach of has been developed to add locale atmosphere interaction to the family of fire area simulators. Numerical coupling of a fire model with an atmospheric model has already been the subject of numerous studies, starting from the work (with static fire) of Heilman and Fast (1992) to the more recent work of Clark *et al.* (2004), that proposes a simplified model of fire spread tailored for a Canadian forest (Rothermel, 1972), coupled with the WRF meso-scale model (Skamarock and Klemp, 2007). While these efforts are effective at simulating the coupled effects at the scale of a large fire (several square kilometres) with a high degree of fire front precision, the use of Rothermel model may be subject to caution as effects of wind and slope to the rate of spread is expressed as coefficients that are experimentally fitted to wind values *as if the fire was not there*.

Other studies are more focused on combustion processes with a detailed physical formulation of the fire front. With WFDS, Mell *et al.* (2006) obtained a good numerical correspondence with real prescribed burning experiment of Australian grassland (Cheney and Gould, 1995). HIGRAD/FIRETEC, Linn *et al.* (2002) is able to perform several numerical investigations with different topography and wind conditions. These efforts are necessary to understand the mechanisms driving the fire spread and to evaluate fire suppression practices. Nevertheless the real-time tracking analysis of large fires

would require access to large computing facilities and detailed ground data, which are difficult to gather because of the scales on which the simulation would be run.

Méso-NH and ForeFire that have been developed to serve research purposes for operational models. In an approach similar to Clark *et al.* (2004), this meso-scale atmospheric model and the reduced physical front tracking wildfire model are coupled to investigate the differences induced by the atmospheric feedback in terms of propagation speed and behaviour. The main originalities of this combination resides in the fact that Méso-NH is run in a Large Eddy Simulation (LES) configuration and that the rate of spread model used in ForeFire provides a physical formulation to take into account effect of wind and slope.

2. Numerical models and coupling method

The coupled code is decomposed into three model components and a coupling component. The atmospheric model is responding to energy fluxes from the fire front. The fire rate of spread model and the front tracking method are used to simulate the fire front at a higher resolution than the atmospheric model. The coupling component performs the simulation synchronisation and the data transformation and interpolation.

Fire propagation model

The fire ROS model is based under the assumption that the flame is acting lake a radiant tilted panel that is heating the vegetation in front of it (see Balbi *et al.*, 2009). It has been developed to provide an analytical formulation of the propagation speed given a slope, wind speed, and fuel parameters. This hypothesis is similar to the hypothesis made by Rothermel model (Rothermel, 1972). Calculations of the flame tilt angle [redacted] given by

$\tan\gamma = \tan\alpha + \dfrac{U}{u_0}$ Is a key point in the model formulation as angle provides the accelerated ROS.

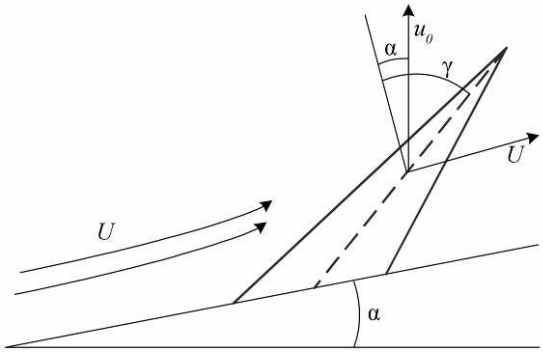

Fig. 1. Calculation of the flame tilt angle.

Figure 1 presents the flame tilt calculation, [redacted] the local slope angle in degrees, *U* the normal wind velocity in the propagation direction (in m.s^{-1}). *R*, the RoS (in m.s^{-1}), is obtained by adding the nominal speed of the fire, to the accelerated speed due to the tilted flame radiating in the direction of the propagation. *R* is given by:

$$R = R_0 + A\frac{R(1+\sin\gamma-\cos\gamma)}{1+\dfrac{R}{r_0}\cos\gamma}.$$

A is a radiant factor (*A* is high if much of the energy generated by combustion is radiated by the front). Parameter r_0 is a speed factor due to radiation (in m.s^{-1}), that is dependent on the flame thickness. Parameter R_0 is the rate of spread without wind and slope (in m.s^{-1}) and u_0, the vertical gas velocity in the flame without wind and slope (in m.s^{-1}).

A front tracking method of markers is used for the simulation of the fire area evolution. The fire line is decomposed into a set of connected points, or markers. Each marker has a specific propagation direction and speed, such as shown in figure 2. The speed at which the marker is travelling along its

propagation vector is given by the rate of spread model. The direction of the propagation vector is taken as the bisector of the angle formed by the marker, and the location of the immediate left and right markers. Markers are redistributed along the front if separated by more than the resolution distance Δr and removed if separated by less than $\Delta r/4$. A fireline is defined as a full set of interconnected markers. Id two points of different firelines are separated by less than $\Delta r/4$ the two fronts are merging. The integration of a marker advance is performed in a discrete event fashion, with no global time step but specific activation time for markers. Every marker is always advancing by the same distance Δq estimating from the propagation speed when the marker would have moved by this distance. The timed activations events are placed in a sorted event list, and the simulation is performed by activating the most imminent event. The method has been selected because of its computational efficiency, and the ability to simulate the propagation of an interface at the high resolution (a few meters) needed to take into account different vegetations, roads, houses and fire breaks over a large area typical of a wildfire accident (hundreds of square kilometres).

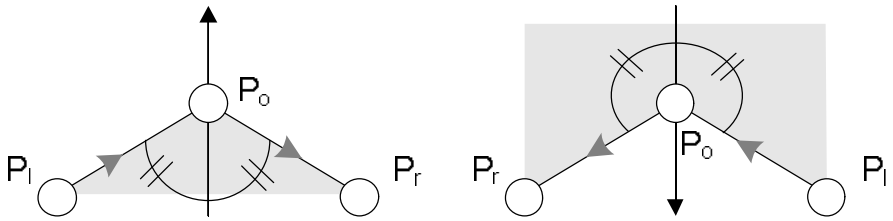

Fig. 2. Front tracking and markers. Circles represent markers along the fire line. Arrows show the propagation vector (bisector of the local angle at the marker P_0 between the point at left, P_l and point at right, P_r). Grey area represents the burned fuel.

The fire front thickness is constructed by projecting the projecting the location of the marker along the propagation vector after the burning duration of the fire, noted R_T for `Residence time_ (see fig. 3).

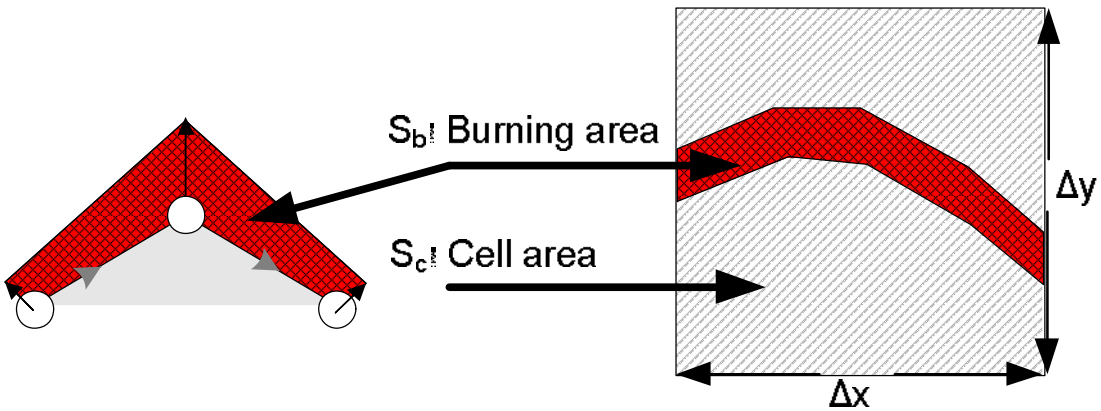

Fig. 3. Integration of burning area. Red shape represents the fire front. Integration is performed on each atmospheric cell (shades of grey correspond to burning (S_b) to total cell area ($S_c = \Delta x \Delta y$) ratio, black is S_b max).

Wind and elevation fields are interpolated at the location of the marker using a bi-cubic method at the very location of the markers. The wind is estimated from the value interpolated at the marker location, while the slope angle in the fire propagation direction is estimated from the elevation difference between the elevation at the fire marker and the elevation at the location projected after R_T.

Meso-NH atmospheric model

This anaelastic non hydrostatic mesoscale model (Lafore *et al.*, 1998) is intended to be applicable to all scales ranging from large (synoptic) scales to small (large eddy) scales and can be coupled with an

on-line atmospheric chemistry module. For the fire coupling application Méso-NH is run in Large Eddy Simulation configuration (Δx <= 50m) mode without chemistry. Turbulence parameterization is based on a 1.5-order closure (Cuxart *et al.*, 2000), with a prognostic equation for turbulent kinetic energy in 3D. We selected open boundary condition for all tests. Momentum variables are advected with a centered 4th order scheme, while scalar and other meteorological variables are advected with a so-called monotonic Piecewise Parabolic Method (Woodward and Colella, 1984). An externalised surface module is used for the fire feedback in the simulation.

Coupling atmospheric and wildfire model

The wildfire model force the atmospheric model at the first (ground) level injecting heat fluxes in W.m^{-2}, flux of water vapour in kg.m^{-2} and radiant temperature in K. Polygon clipping is used to derive the burning surface of an atmospheric cell, (noted S_b) over the total cell area noted S_c ($\Delta x \Delta y$) (Figure 3). The burning ratio for each atmospheric grid cell is noted R_b, = S_b / S_c.

As only a portion of the cell is burning, an equivalent radiant temperature (T_e) for the whole cell is averaged from a nominal flame temperature (T_n) and the soil temperature from the atmospheric model (T_s). T_e is given by:

$$T_e = \sqrt[4]{(1-R_b)T_s^4 + R_b T_n^4} \ ,$$

Equivalent heat fluxes (Q_e) in W.m^{-2}, corresponding to the energy of the hot gaseous column over an atmospheric cell, is approximated from a nominal convective heat flux (Q_n) with $Q_e = R_b Q_n$.

Finally, equivalent water vapour fluxes (Wv_e) in kg.m^{-2}, representing the amount of water vapour evaporated from the vegetation is interpolated over an atmospheric cell from nominal water vapour content (Wv_n) with $Wv_e = R_b Wv_n$.

The operation is performed for all atmospheric grid point at ground level, allowing to construct three matrices that are passed to the atmospheric model just before just before updating the wind matrix used by the fire simulation. Wind matrices forcing the fire model are updated at each atmospheric time step and wind is assumed to be constant during the entire duration of the step.

3. Experimental Set-up and simulation results.

In order to evaluate the ability of the coupled code to estimate the coupled influences of topography and wind on fire spread, 5 tests were ran corresponding to a partial set of the set-ups proposed by Linn *et al*. (2007). Base functions used to create the different topographies are from Linn *et al*. (2007), those functions are used to create an idealized flat, canyon, hill ridge and up can terrain.

For all cases the domain size has been set to 640*320*500m with horizontal spacing of 8m and an average vertical spacing of 10m. Vegetation is assumed homogeneous, with parameters (Table 1) for all simulations, based on mean values deduced from experimental studies (Santoni *et al.*, 2006). In this experiment, vegetation was shrubs with an average dry fuel load of 7 kg.m^{-2}.

A	R0	r0	u0	R_T.	Q_e.	Wv_e	T_n
1.5	0.1m.s^{-1}	0.01m.s^{-1}	5m.s^{-1}	30s	250kW.m^{-2}	0.1kg.m^{-2}	1000K

Table 1. Experimental parameters, with *A*: Radiant factor, R_0: rate of spread without wind and slope, r_0 flame thickness speed factor, u_0: flame gas velocity, R_T: fire residence time, Q_n: nominal heat flux, Wv_n: nominal water vapour flux and T_n: nominal radiant temperature.

Atmospheric model background wind field was of 6m.s^{-1} constant in height (with a maximum simulation height of 500m). A passive scalar tracer with a distribution set to the burning ratio of each grid point and for each atmospheric time step is used as a marker for smoke injection.

Figures 4, 5, 6, 7, and 8 present the simulation results for the flat, canyon, hill, ridge and upcan cases 120s after ignition. In the flat Case (Fig 4 a) the flow remains largely unaffected behind the fire. The simulation reveals an area of confluence ahead of the front with some recirculation that is located at the base of the fire plume (Fig 4 b). The plume is relatively weak, affecting the flow to an altitude of 100m over ground. Overall flow speed does not greatly differ from the original flow speed of 6m.s^{-1}.

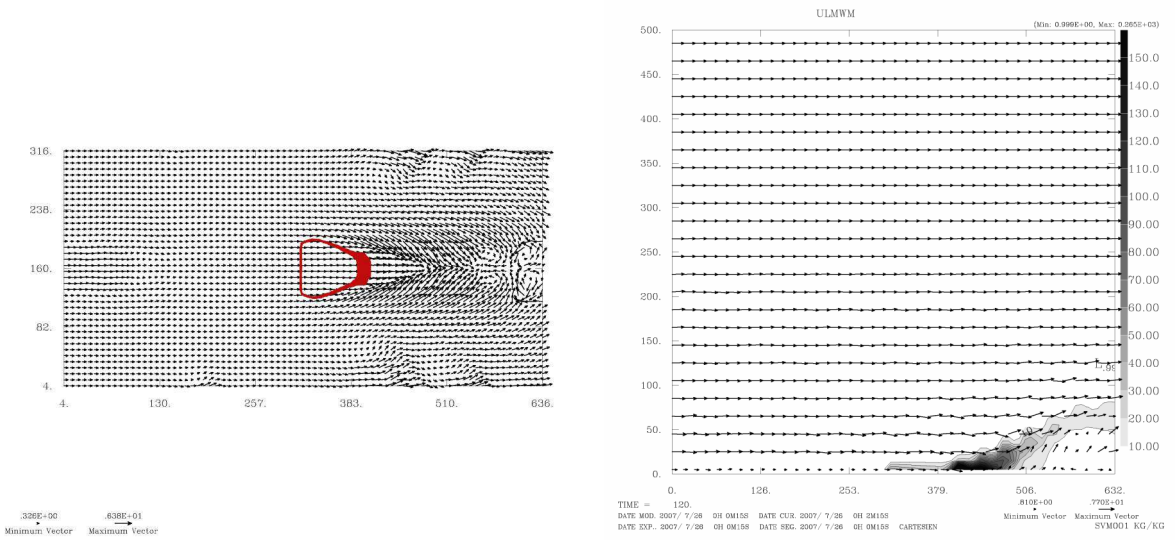

Fig. 4. FLAT (a) Horizontal section (x/y) at Z=10m, fire lines after 120 seconds of simulation. Arrows denote the wind vectors at ground level. (b) Cross section (x/z) of the coupled case at Y=160m, shading represents concentration of the injected passive tracer.

Situation is different in the canyon case (Figure 5) where the flow speed at ground level is accelerated to13m.s^{-1} .

The accelerated flow, combined with a steep slope does greatly accelerate the fire rate of spread. Nevertheless, as can be seen in Figure 4(b) the area of convergence is situated just over the fire head, providing weaker winds to tilt the flame. It appears that the canyon topography is creating a recirculation, visible Figure 4(b) that is weakening the winds at ground level near the front.

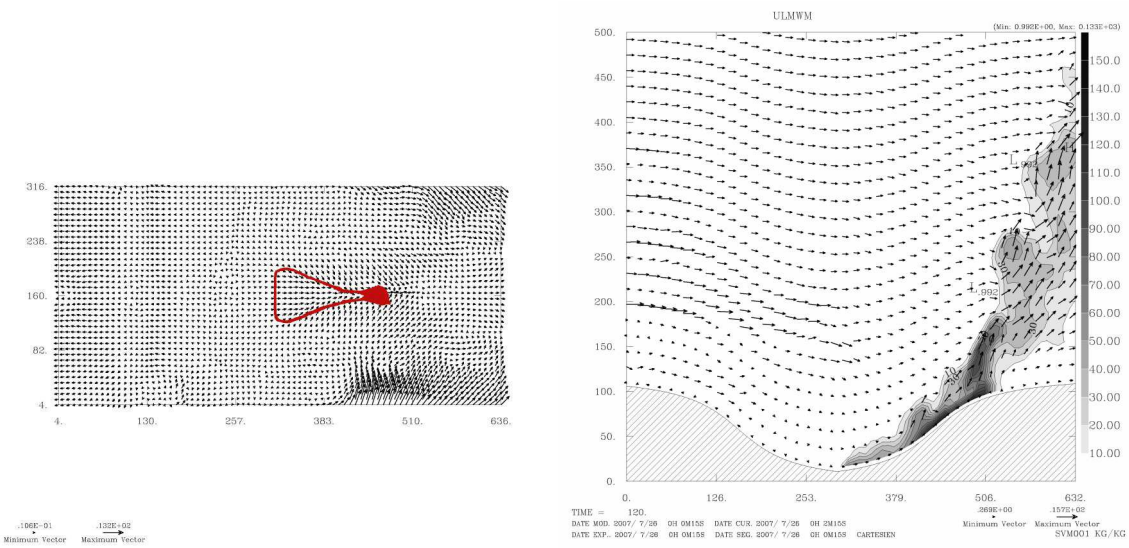

Fig. 5. CANYON (a) Horizontal section (x/y) at Z=10m, fire lines after 120 seconds of simulation. Arrows denote the wind vectors at ground level. (b) Cross section (x/z) of the coupled case at Y=160m, shading represents concentration of the injected passive tracer.

Wit the same slope and same wind speed, the Hill case (Figure 6) presents a different behaviour. The area of confluence is located here ahead of the fire front, so the maximum wind speed are just over the fire head. The resulting tilt angle results in a stronger ROS, and a larger burning injection area.

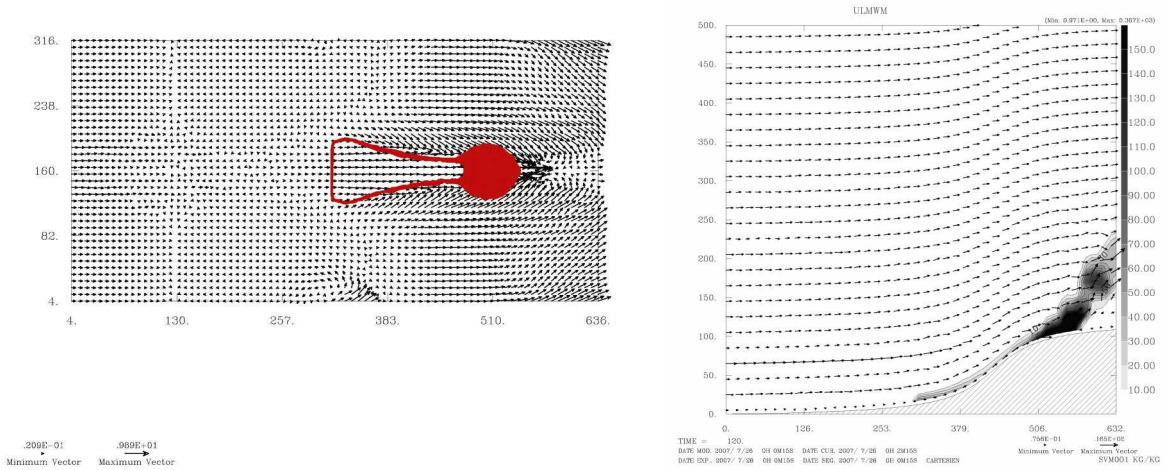

Fig. 6. HILL (a) Horizontal section (x/y) at Z=10m, fire lines after 120 seconds of simulation. Arrows denote the wind vectors at ground level. (b) Cross section (x/z) of the coupled case at Y=160m, shading represents concentration of the injected passive tracer.

The ridge case (Figure 7) is similar to the hill case; a specificity of this case is that locally, over the ridge, wind is accelerated over the flank, creating bursts of fire and a less regular fire shape.

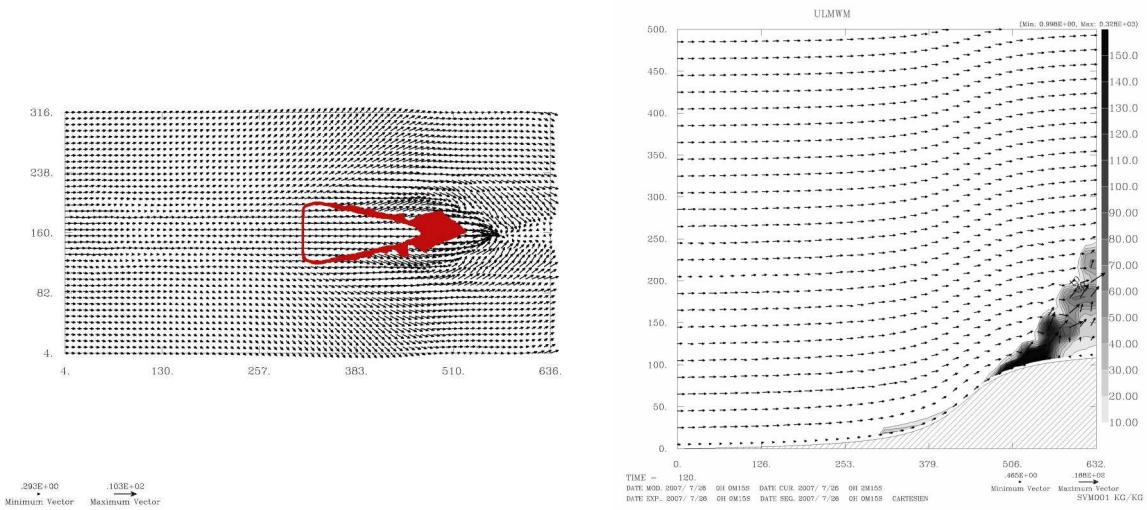

Fig. 7. RIDGE (a) Horizontal section (x/y) at Z=10m, fire lines after 120 seconds of simulation. Arrows denote the wind vectors at ground level. (b) Cross section (x/z) of the coupled case at Y=160m, shading represents concentration of the injected passive tracer.

Finally the Upcan case (Figure 8) that has no clear area of convergence ahead of the front. Because of the specific topography, the flow is not creating a hot column, but is moving towards the flank generating a large area of injection with lower local concentration (Figure 8(b)). Nevertheless, the wind is still strong near the fire head, accelerating the front to ROS comparable to the ridge or canyon cases.

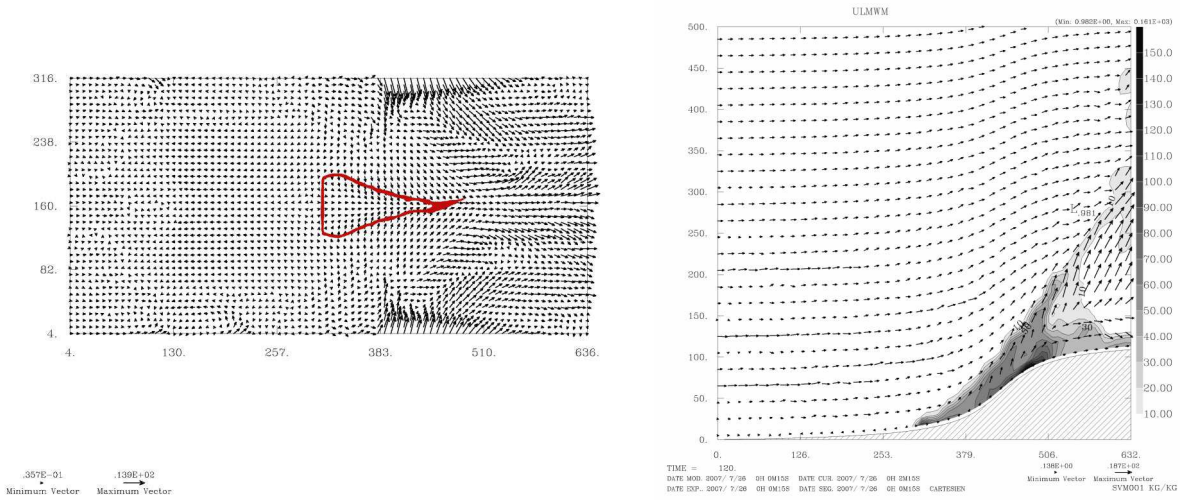

Fig. 8. UPCAN (a) Horizontal section (x/y) at Z=10m, fire lines after 120 seconds of simulation. Arrows denote the wind vectors at ground level. (b) Cross section (x/z) of the coupled case at Y=160m, shading represents concentration of the injected passive tracer.

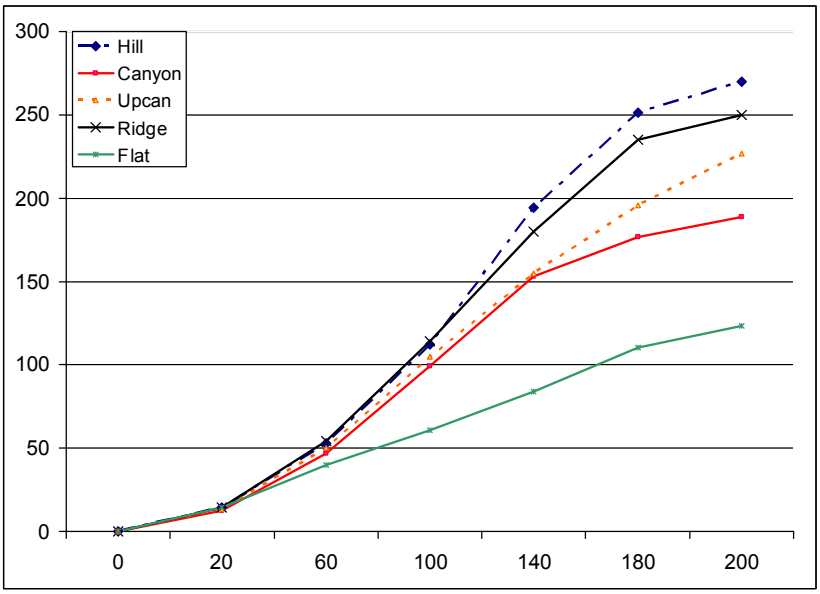

Fig. 9. Time (0 to 300 s) to the front head position (between 0 and 200m).

Figure 9 presents the position of the fire head over time. We can observe that for the Hill and Ridge cases, a strong acceleration is happening 60 meters after the starting point, corresponding to the start of the steep slope, this acceleration ends at 180m, corresponding here to the end of the steep slope. The Upcan case is less affected by the slope effect, as the slope is less abrupt in this case, nevertheless, in this case, the propagation speed does continue to stay at almost its maximum level until the end of the domain, suggesting that the flow, accelerated by the fire, is still influencing heavily the fire spread (figure 8 a).

The Canyon case is exactly the same slope as the Hill case; however, Figure 9 clearly shows that the spread behaviour is different here. In Figure 5 we can observe that the canyon topography generates a horizontal recirculation that is preventing strong flow to reach the fire head and creates a reverse flow near the bottom of the Canyon. Similar behaviour is present in the simulation from Linn *et al*. (2007) with HIGRAD/FIRETEC, although it is not possible to state that the same effects are involved.

Finally, the flat case spread rate is almost constant during the whole simulation run, and less affected by the coupled atmospheric effects.

All simulations were performed on a bi dual-core Intel Xeon processor running at 3 Ghz with 8Gb of memory. The calculation time for each run was about 4 hours for 300 seconds of simulation with a

time step of 0.1s. The calculation of the fire front displacement only accounts for 10 seconds of computer time, while the coupling requires 200 seconds of mainly input/output operations for the whole duration of the run.

4. Conclusions

MésoNH-ForeFire coupled model of wildland fire spread is used to investigate the effect of topography on fire induced winds. With a straightforward coupling method, the atmospheric model is able to simulate the atmosphere dynamic induced by the fire and the subsequent effects on the RoS with meaningful results. The five idealized scenarios allowed simulating induced flow patterns similar to those observed from the simulation by Linn *et al*. (2007) with HIGRAD/FIRETEC. Another important aspect of these simulations is that the fire head spread rate is also comparable to those found by Linn *et al*. (2007), significantly lower in the Flat scenario, and slightly lower in the canyon case. Nevertheless, unlike HIGRAD/FIRETEC, performing simulation of the flow and fire patterns over a complex vegetation distribution at a high resolution is impossible with the proposed coupled model. The objective was here to move from fire area model with forced wind fields to coupled wind field that could represent the local perturbations that may greatly affect fire behaviour. Further enhancements are planned to perform simulation of large past fire and simulation with the online chemistry module of Méso-NH to investigate fire smoke and particle transport.

Acknowledgements

This research was supported by PEPS- 07_36 from the French National Centre of Scientific Research (CNRS).

References

Balbi JH, Rossi JL, Marcelli T, Santoni PA, (2007) A 3D physical real-time model of surface fires across fuel beds, Combustion Science and Technology, 179, 2511-2537. doi:10.1080/00102200701484449

Clark, T. L., Jenkins, M. A., Coen, J., Packham, D., 1996: A Coupled Atmospheric-Fire Model: Convective Froude number and Dynamic Fingering. International Journal of Wildland Fire, 6, 177-190. doi:10.1071/WF9960177

Clark, T.L., Coen, J., Latham, D.:(2004), Description of a coupled atmosphere-fire model, International J. of Wildland Fire, 13, 49¯63. doi:10.1071/WF03043

J. L. Coen, T. L. Clark, and D. Latham. Coupled atmosphere-fire model simulations in various fuel types in complex terrain. In 4th. Symp. Fire and Forest Meteor. Amer. Meteor. Soc., Reno, Nov. 13-15, pages 39--42, 2001.

Cuxart, J., Bougeault, Ph. and Redelsperger, J.L., 2000: A turbulence scheme allowing for mesoscale and large-eddy simulations. Q. J. R. Meteorol. Soc., 126, 1-30.

Heilman WE, Fast JD (1992) Simulations of Horizontal Roll Vortex Development Above Lines of Extreme Surface Heating. International Journal of Wildland Fire 2, 55¯68. doi:10.1071/WF9920055

Lafore, J. P., J. Stein, N. Asencio, P. Bougeault, V. Ducrocq, J. Duron,C. Fischer, P. Hereil, P. Mascart, J. P. Pinty, J. L. Redelsperger, E. Richard, and J. Vila-Guerau de Arellano, 1998: The Meso-NH Atmospheric Simulation System. Part I: Adiabatic formulation and control simulations. Annales Geophysicae, 16, 90-109. doi:10.1007/s00585-997-0090-6

Linn, R.R., Reisner, J., Colman, J., Winterkamp, J. (2002), Studying Wildfire Using FIRETEC, International Journal of Wildland Fires, 11, 1-14. doi:10.1071/WF02007

Linn RR, Winterkamp J, Edminster C, Colman JJ, Smith WS (2007) Coupled influences of topography and wind on wildland fire behaviour. International Journal of Wildland Fire 16, 183¯195. doi:10.1071/WF06078

Masson V. 2000, A physically based scheme for the urban energy budget in atmospheric models, Bound. Layer Meteor., 94, 357-397. doi:10.1023/A:1002463829265

Mell, W., Jenkins, M.A., Gould, J., Cheney, P.: (2007), :A physically based approach to modelling grassland fires˘, International J. of Wildland Fire, 16, 1--22. doi:10.1071/WF06002

Noilhan, J. and S. Planton, 1989: A simple parameterization of land surface processes for meteorological models. Mon. Weather Rev., 117, 536-549. doi:10.1175/1520-0493(1989)117<0536:ASPOLS>2.0.CO;2

Santoni PA, Simeoni A, Rossi JL, Bosseur F, Morandini F, Silvani X, Balbi JH, Cancellieri D, Rossi L (2006) Instrumentation of wildland fire: characterisation of a fire spreading through a Mediterranean shrub, Fire Safety Journal, 41(3) 171-184. doi:10.1016/j.firesaf.2005.11.010

Skamarock, W. C., J. B. Klemp, (2007), A Time-Split Nonhydrostatic Atmospheric Model for Research and NWP Applications. J. Comp. Phys. special issue on environmental modeling. Volume 227, Issue 7.

Rothermel R (1972). A mathematical model for predicting fire spread in wildland fuels. Research Paper INT-115, USDA Forest Service.

Woodward, P.R. and P.Colella, 1984 : The piecewise Parabolic Method (PPM) for gas dynamical simulations, J. Comput. Phys., 54, 174-201. doi:10.1016/0021-9991(84)90143-8